Whale Optimization Algorithm Based Closed-Loop Control Z-source Inverter for Wind Energy Application

Sweta Kumari[†] and **Rajib Kumar Mandal**, Non-members

ABSTRACT

In this paper, an enhanced 0.5 kW Z-source inverter (ZSI) model is used in the design of a wind energy generating system (WEGS) that uses a 1.2 kW wind turbine to overcome the operating restrictions of the traditional ZSI model. To achieve a constant line-to-line voltage with varying loads at the output side of the WEGS, a closed-loop control technique is applied at the load side. A proportional-integral (PI) controller is utilised with the ZSI for closed-loop control since it is the least complicated in terms of tuning and operation. Also, ZSI systems have nonlinear behaviour, which precludes direct application of the PI controller technique to them. As a result, the novelty of this article is the optimisation of stabilised PI coefficients (Kp, Ki) with a modified ZSI model. Particle swarm optimisation (PSO), sine-cosine algorithm (SCA), and whale optimisation algorithm (WOA)-based optimisation techniques are used to handle PI tuning for closed-loop modified ZSI. In terms of the stability of the closed-loop modified ZSI with WEGS, the WOA performs better. The outcomes show that the suggested controller can control the variation in AC output voltage of ZSI with variable load exactly.

Keywords: Proportional-Integral (PI) Controller, Simple Boost Pulse-Width-Modulation (SB-PWM), Whale Optimisation Algorithm (WOA), Wind Energy Generation System (WEGS), Z-Source Inverter (ZSI).

1. INTRODUCTION

The current situation is struggling to reduce greenhouse gas emissions and increase energy efficiency. The best alternative solution to this problem is renewable energy (RE). To make the RE system effective and cost-friendly, integration of RE with ZSI is advantageous as it reduces the component count in the system as well as the complexity of the system [1], [2]. However, the three-phase ZSI has many advantages, like fast transient response, better steady-state performance, utilisation of the shoot-through state, etc [3]. Thus, it has become of interest to researchers.

Although ZSI has many favourable advantages, it also has some drawbacks [4]. The main problem associated with the ZSI is the greater capacitor voltage than the input DC voltage. Also, the Z-source inductors' start-up inrush current cannot be suppressed, resulting in a current surge that could endanger the devices. These limitations of traditional ZSI are overcome by the modified model of ZSI discussed in detail in Section 2.

ZSI offers a number of positive benefits, although its effectiveness mostly depends on control techniques: feedback control and PWM [5]. There are many cases where the issue is considered a control factor. PID and PI controllers are frequently utilised when it comes to controlling the capacitor voltage of ZSI's impedance network. As a consequence of this fact, there has been considerable detailed research into PI and PID controllers [6]–[8]. It seems simple to understand and use the PI controller. Because there are only two design parameters—Kp (proportional) and Ki (integral), engineers still prefer the PI controller for ZSI control operation [9].

The construction of PI's parameters for ZSI structures is a compelling topic, despite the fact that it is an efficient control approach. Moreover, due to the nonlinear behaviour of ZSI systems, this control strategy is not directly applicable to these systems. The best value for the controller parameters, however, is not the main focus of research in the aforementioned literature. The issue of computing PI and PID controller parameters is seen as an optimisation problem. Using well-known heuristic techniques such as the genetic algorithm [10], particle swarm optimisation (PSO) [11], and others [12], these parameters are calculated. However, these optimisation techniques are not cast for non-linear ZSI closed-loop control.

This paper focuses on the control strategy for a modified model of ZSI for constant load voltage with a WEGS, and a meta-heuristic algorithm (WOA) is introduced for the optimisation of controller gain parameters.

The WOA algorithm outperforms other comparable algorithms in terms of cost optimisation and preserving voltage stability. Because WOA only saves global optimal values during iteration, it uses less storage space [13]. Due to the existence of two mathematical formulas that can be used to alter the solution path's constituents,

Manuscript received on November 14, 2023; revised on March 28, 2024; accepted on April 8, 2024. This paper was recommended by Associate Editor Chainarin Ekkaravarodome.

The authors are with National Institute of Technology Patna, India.

[†]Corresponding author: swetak.phd18.ee@nitp.ac.in

Digital Object Identifier: 10.37936/ecti-eec.2024222.251270

the random selection of the WOA algorithm is more reliable than the other algorithms. As a result, the WOA algorithm is chosen as the meta-inspired technique in this paper. WOA is more effective than a number of other well-known algorithms, such as Particle Swarm Optimisation (PSO) [14], [15], and Sine Cosine Algorithm (SCA) [16], [17], for avoiding and exploiting local solutions.

Moreover, ZSI's shoot-through (ST) duty ratio (DST) regulates the DC link voltage to maintain the stability of the output voltage. With direct control techniques, the controller controls the shoot-through duty cycle in response to changes in inverter DC-link voltage. Also, the capacitor voltage of ZSI (V_C) controls the DC-link voltage directly. Finding a transfer function between capacitor voltage and ST state duty ratio is therefore necessary. Consequently, in this article, a small signal analysis of ZSI is carried out.

The following are the primary contributions to this paper:

1. A simulation model of a ZSI is designed with its impedance network parameters, i.e., impedance network inductance (L_{ZSI}) and capacitance (C_{ZSI}), set such that there is no resonance in the inverter network.
2. The mathematical, or state-space model, of the ZSI network is analysed in terms of state variables and input functions.
3. A proper modulation technique for a ZSI is found and utilised to get less % THD at the AC output side of the inverter.
4. The whale optimisation technique is analysed, and a flow chart for controller parameter design is mapped.
5. The response of the system with the optimised PI controller is analysed.

The remaining organisation of this article is as follows: Section 2 describes the ZSI as well as the modified ZSI structure and parameters. Section 3 discusses the modulation technique for a ZSI with WEGS. Section 4 shows the ZSI state space model with controller design. Also, the transfer function between the voltage of the Z source capacitor and the shoot-through duty ratio is determined. Section 5 describes the WOA with its flow chart, then Section 6 is the result and discussion section.

2. Z-SOURCE INVERTER

The proposed WEGS incorporating ZSI circuit model is shown in Fig. 1. The conventional WEGS need the use of a transformer or a DC-DC chopper to raise the system's voltage level. This complicates the system. In contrast, ZSI has excellent performance to lower the component count in integration with any RE source generation system.

2.1 Design of a ZSI

The structure of the cross-coupled network of ZSI is shown in Fig. 1. The voltage across the capacitor and the voltage across the inductor are the same when considering L_1=L_2=L_{ZSI} and C_1=C_2=C_{ZSI}. The values of capacitors and inductors are determined by the ripple voltage of the capacitor and the ripple current of the inductor, respectively. Thus, choosing the appropriate values for the capacitor and inductor affects the performance of a ZSI [18].

***Table 1**: Parameters for ZSI design.*

ZSI Parameters	Value
DC input voltage (V_{in})	36 V
Inductor (L_1=L_2=L_{ZSI})	1.5 mH
Capacitor (C_1=C_2=C_{ZSI})	1000 µF
RMS line-to-line voltage	91 V
Switching frequency (f)	6000 Hz
Inverter filter capacitance	220 µF
Inverter filter inductance	1000 µH

$$C_{ZSI} \geq \frac{D_{ST} I_L}{2f\Delta V_C} \tag{1}$$

$$L_{ZSI} \geq \frac{D_{ST} V_C}{2f\Delta I_L} \tag{2}$$

where D_{ST} is the ST duty ratio. I_L and V_C are the average current through the inductor and the average voltage across the capacitor, respectively. f is the switching frequency of switches of the main ZSI switching circuit. ΔV_C and ΔI_L are ripple voltage across the capacitor and ripple current through the inductor, respectively. Considering the above conditions, the ZSI of 0.43 kW, 91 V, and 50 Hz is modelled. The different parameters for the ZSI design are listed in Table 1.

2.2 ZSI Operation

The third-state ST state of operation is introduced in ZSI operation, along with the active and zero states of traditional inverters [19]. There are now two operating conditions for ZSI: the ST state and the non-ST state. Ordinarily, it is observed that the two inductors are charged in ST mode and discharged in non-ST mode.

Both inductors offer energy with DC input voltage (V_{in}), and hence there is boosting of DC link voltage or inverter input voltage (V_{DC}). Hereafter, the boosting voltage level depends on the time period of the ST state.

Assuming D_{ST} is the duty ratio of the ST mode of operation, then the boost factor (B_{ZSI}) of ZSI, by the circuit operation, can be represented as:

$$B_{ZSI} = \frac{1}{1 - 2D_{ST}} \tag{3}$$

Also, the inverter input voltage (V_{DC}) and the phase voltage of the AC output (V_{AC}) can be written as the modulation index (M_I) of the inverter:

$$V_{DC} = B_{ZSI} \cdot V_{in} = \frac{V_{in}}{1 - 2D_{ST}} \tag{4}$$

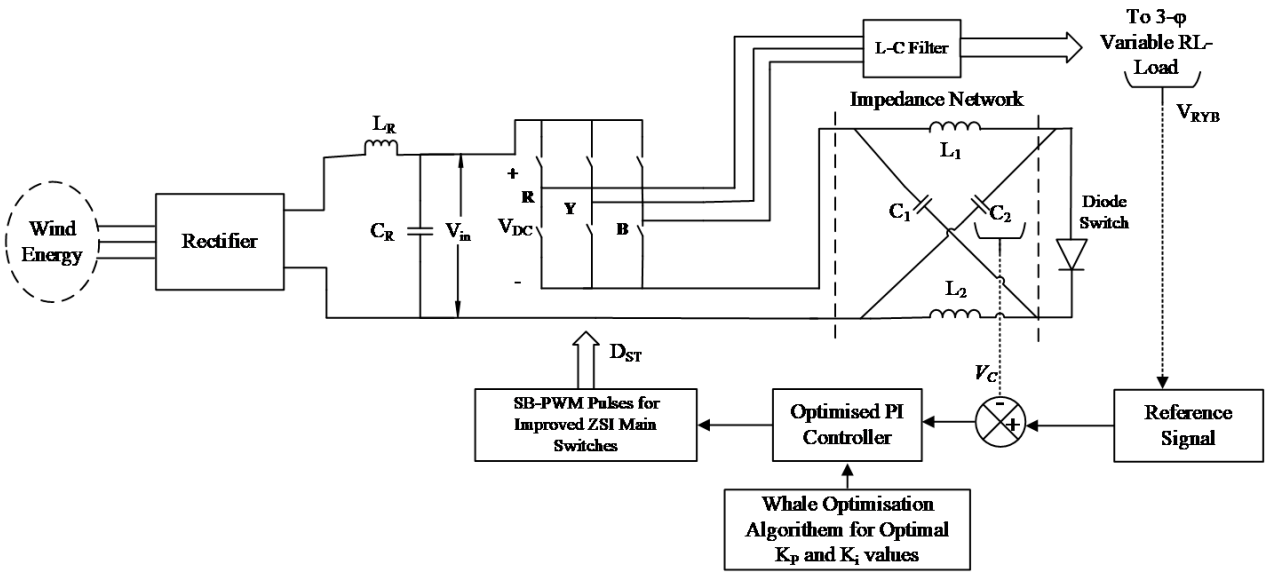

***Fig. 1**: Proposed WEGS model with closed-loop ZSI and variable RL-load.*

$$V_{AC} = M_I \cdot V_{DC} \tag{5}$$

Equation (5) demonstrates how the B_{ZSI} and M_I of the inverter will both affect the ZSI's output AC voltage.

2.3 Modified Model of ZSI

Together with the above-described advantages, the conventional ZSI topology has the following issues: a) The voltage across C_{ZSI} is greater than the V_{in}; in this way, high-voltage capacitors ought to be utilised, which might bring about a bigger volume and end up being costly to the network; b) Z-source inductors' start-up inrush current is very large, resulting in a current surge that could risk the devices [20].

A new ZSI topology is presented to address the downsides of the traditional ZSI. Fig. 2 depicts the modified ZSI model. The components used in modified model are identical to those in the previous version only the diode and inverter bridge are in different places because their positions are swapped and their directions of connection are reversed. In the proposed topology, C_{ZSI} maintains the voltage at or below the input voltage (V_{in}); consequently, for the same voltage increase, the capacitor voltage stress can be significantly reduced. Additionally, in comparison to the prior topology, this one possesses an inherent capability for inrush-current limitation.

3. MODULATION TECHNIQUE FOR ZSI

The ZSI's DC link voltage and boost factor are not sufficient to provide a desirable output AC voltage. Many modulation techniques for ZSI with WEGS have been examined in [21]. The simple boost pulse width modulation (SB-PWM) is much suited for ZSI in the WEGS system [21].

This method is based on a comparative analysis of a three-sinusoidal line and a triangular carrier wave.

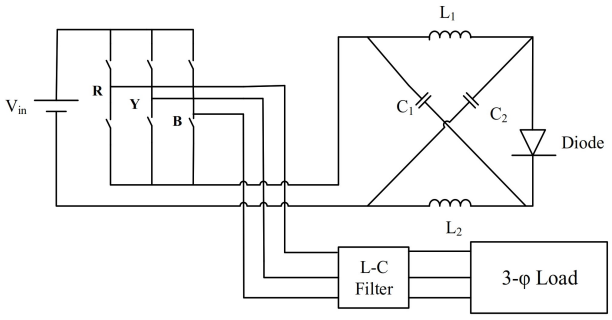

***Fig. 2**: Modified ZSI model with filter and three-phase load.*

Although ZSI needs to generate ST pulses for the switching circuit, in the SB-PWM method, ST pulses are generated with the help of DC lines [22] [23]. For SB-PWM, there is a limitation to the duty ratio (D_{ST}), is ($1\text{-}M_I$).

4. STEADY STATE ANALYSIS OF ZSI

This article presents a complete average model of ZSI with RL load using the state space model. A system's state space representation can be expressed as:

$$G\nabla\, x(t) = a' x(t) + b' u(t) \tag{6}$$

$$y(t) = c' x(t) + d' u(t) \tag{7}$$

where, ∇ = d/dt

As a matrix, G contains the capacitance and inductance values. The state vector is $x(t)$. $x(t)$ contains the state variables. The voltage across the capacitor (v_C) and the current that flows through the inductor network (i_L) are the state variables. $u(t)$ is the input vector; it contains the input source (V_{in}). The linear combination of the elements $u(t)$ and $x(t)$ is expressed as $G\nabla$ x (t).

These a', b', c' and d′are the proportionality constants. Also, the linear combination of $x(t)$ and $u(t)$ is the output vector $y(t)$.

The switching time period T ($1/f$, the system's switching frequency is a lot more than natural frequency, i.e., 50 Hz) can be divided into two sub-intervals [24]:

- ST state duration $0 \leq t \leq T_{ST}$ (T_{ST} is the ST time period). The state space equations for this interval are:

$$G\nabla\, x(t) = a'_1 x(t) + b'_1 u(t) \tag{8}$$

$$y(t) = c'_1 x(t) + d'_1 u(t) \tag{9}$$

- Non-ST state duration $T_{ST} \leq t \leq T$. The state space equations for this interval are:

$$G\nabla\, x(t) = a'_2 x(t) + b'_2 u(t) \tag{10}$$

$$y(t) = c'_2 x(t) + d'_2 u(t) \tag{11}$$

The equation that defines the ZSI in steady state is the averaging state space model:

$$0 = a'X + b'U \tag{12}$$

$$Y = c'X + d'U \tag{13}$$

The average model matrices are:

$$a' = a'_1\, D_{ST} + a'_2\, M_I \tag{14}$$

$$b' = b'_1\, D_{ST} + b'_2\, M_I \tag{15}$$

$$c' = c'_1\, D_{ST} + c'_2\, M_I \tag{16}$$

$$d' = d'_1\, D_{ST} + d'_2\, M_I \tag{17}$$

where, U = input DC vector in steady state, X = DC vector in steady state, Y = output DC vector in steady state, and D_{ST} = Duty cycle in steady state.

$$M_I = 1 - D_{ST}$$

By solving (12) and (13) we can write:

$$X = -\frac{b'U}{a'} \tag{18}$$

$$Y = -\frac{c'b'U}{a'} + d'U \tag{19}$$

Equation (20) represents the AC small signal state equation:

$$G\nabla\tilde{x}\,(t) = a'\tilde{x}(t) + b'\tilde{u} + \left[\left(a'_1 - a'_2\right)X + \left(b'_1 - b'_2\right)U\right]\tilde{d}(t) \tag{20}$$

$$\tilde{y}\,(t) = c'\tilde{x}(t) + d'\tilde{u}(t) + \left[\left(c'_1 - c'_2\right)X + \left(d'_1 - d'_2\right)U\right]\tilde{d}(t) \tag{21}$$

Here $\tilde{x}\,(t)$, $\tilde{u}\,(t)$, $\tilde{y}\,(t)$, and $\tilde{d}(t)$ is the quantities of small variation AC in the steady-state solution. From equations (8) to (11) shows the state space representation of the inverter, and from equations (12) to (21) used to derive the AC small signal model.

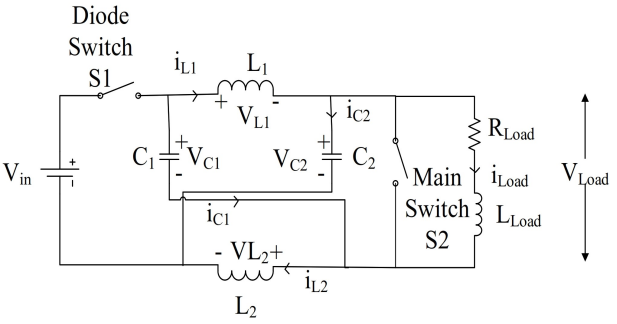

***Fig. 3**: Equivalent ZSI model.*

As there are symmetric network in ZSI's impedance network, hence three state variables present in ZSI:

- Voltage across capacitor in impedance network (v_C)
- Current through inductor in impedance network (i_L)
- Current through the load inductor (i_{Load})

Fig. 3 shows the equivalent circuit model of a ZSI. R_{Load} (resistance/phase) and L_{Load} (inductance/phase) are the AC loads. Switch S_1 is the diode switch responsible for single-direction current flow in ZSI, and switch S_2 is equivalent to a 3-leg inverter's switching system.

Now the state variables can be signified as a vector:

$$x(t) = \begin{bmatrix} i_{L_1}(t) & i_{L_2}(t) & v_{C_1}(t) & v_{C_2}(t) & i_{Load}(t) \end{bmatrix}^T$$

For the ST time period (T_{ST}) equation (8) can be written in the form:

$$\begin{bmatrix} L_1 & 0 & 0 & 0 & 0 \\ 0 & L_2 & 0 & 0 & 0 \\ 0 & 0 & C_1 & 0 & 0 \\ 0 & 0 & 0 & C_2 & 0 \\ 0 & 0 & 0 & 0 & L_{Load} \end{bmatrix} d/dt \begin{bmatrix} i_{L_1}(t) \\ i_{L_2}(t) \\ v_{C_1}(t) \\ v_{C_2}(t) \\ i_{Load}(t) \end{bmatrix}$$

$$= \begin{bmatrix} 0 & 0 & 1 & 0 & 0 \\ 0 & 0 & 0 & 1 & 0 \\ -1 & 0 & 0 & 0 & 0 \\ 0 & -1 & 0 & 0 & 0 \\ 0 & 0 & 0 & 0 & -R_{Load} \end{bmatrix} \begin{bmatrix} \mathrm{i}_{L_1}(t) \\ \mathrm{i}_{L_2}(t) \\ \mathrm{v}_{C_1}(t) \\ \mathrm{v}_{C_2}(t) \\ \mathrm{i}_{Load}(t) \end{bmatrix} \tag{22}$$

where, $G = \begin{bmatrix} L_1 & 0 & 0 & 0 & 0 \\ 0 & L_2 & 0 & 0 & 0 \\ 0 & 0 & C_1 & 0 & 0 \\ 0 & 0 & 0 & C_2 & 0 \\ 0 & 0 & 0 & 0 & L_{Load} \end{bmatrix}$

$$a'_1 = \begin{bmatrix} 0 & 0 & 1 & 0 & 0 \\ 0 & 0 & 0 & 1 & 0 \\ -1 & 0 & 0 & 0 & 0 \\ 0 & -1 & 0 & 0 & 0 \\ 0 & 0 & 0 & 0 & -R_{Load} \end{bmatrix} \text{ and } b'_1 = \begin{bmatrix} 0 \\ 0 \\ 0 \\ 0 \\ 0 \end{bmatrix}$$

Similarly, the state equation for the non-ST state may also be written in the form $G\nabla\, x(t) = a'_2 x(t) + b'_2 u(t)$

from equation (10):

$$\begin{bmatrix} L_1 & 0 & 0 & 0 & 0 \\ 0 & L_2 & 0 & 0 & 0 \\ 0 & 0 & C_1 & 0 & 0 \\ 0 & 0 & 0 & C_2 & 0 \\ 0 & 0 & 0 & 0 & L_{Load} \end{bmatrix} d/dt \begin{bmatrix} i_{L_1}(t) \\ i_{L_2}(t) \\ v_{C_1}(t) \\ v_{C_2}(t) \\ i_{Load}(t) \end{bmatrix}$$

$$= \begin{bmatrix} 0 & 0 & 0 & -1 & 0 \\ 0 & 0 & -1 & 1 & 0 \\ 0 & 1 & 0 & 0 & -1 \\ 1 & 0 & 0 & 0 & -1 \\ 0 & 0 & 1 & 1 & -R_{Load} \end{bmatrix} \begin{bmatrix} \mathrm{i}_{L_1}(\mathrm{t}) \\ \mathrm{i}_{L_2}(\mathrm{t}) \\ \mathrm{v}_{C_1}(\mathrm{t}) \\ \mathrm{v}_{C_2}(\mathrm{t}) \\ \mathrm{i}_{\mathrm{Load}}(\mathrm{t}) \end{bmatrix}$$

$$+ \begin{bmatrix} 1 \\ 1 \\ 0 \\ 0 \\ -1 \end{bmatrix} v_{in}(t) \tag{23}$$

where, $a'_2 = \begin{bmatrix} 0 & 0 & 0 & -1 & 0 \\ 0 & 0 & -1 & 1 & 0 \\ 0 & 1 & 0 & 0 & -1 \\ 1 & 0 & 0 & 0 & -1 \\ 0 & 0 & 1 & 1 & -R_{Load} \end{bmatrix}$

and $b'_2 = \begin{bmatrix} 1 \\ 1 \\ 0 \\ 0 \\ -1 \end{bmatrix}$

Equations (22) and (23) describe the relationship between state variables and input (v_{in}). Equation (24) describes the steady-state state space model based on equations (12), (13) and (14)-(17):

$$\begin{bmatrix} 0 \\ 0 \\ 0 \\ 0 \\ 0 \end{bmatrix} = \begin{bmatrix} 0 & 0 & D_{ST} & -M_I & 0 \\ 0 & 0 & -M_I & D_{ST} & 0 \\ -D_{ST} & M_I & 0 & 0 & -M_I \\ M_I & -D_{ST} & 0 & 0 & -M_I \\ 0 & 0 & M_I & M_I & -R_{Load} \end{bmatrix}$$

$$\begin{bmatrix} I_{L_1} \\ I_{L_2} \\ V_{C_1} \\ V_{C_2} \\ I_{Load} \end{bmatrix} + \begin{bmatrix} M_I \\ M_I \\ 0 \\ 0 \\ -M_I \end{bmatrix} V_{in} \tag{24}$$

where, I_{L_1}, I_{L_2}, V_{C_1}, V_{C_2}, I_{Load} and V_{in} are steady state values. With reference to the equations (12) and (13) for the steady state values of state variables:

$$V_C = \frac{M_I}{M_I - D_{ST}} V_{in} \tag{25}$$

$$I_L = \frac{M_I}{M_I - D_{ST}} I_{Load} \tag{26}$$

$$I_{Load} = \frac{V_C}{R_{Load}} \tag{27}$$

Usually, the small signal perturbation of the state variable is represented by equation (28):

$$x(t) = X + \tilde{x}(t) \tag{28}$$

The reference equation (20) can be used to find the state equation for the small signal AC model [24]:

$$\begin{bmatrix} L_1 & 0 & 0 & 0 & 0 \\ 0 & L_2 & 0 & 0 & 0 \\ 0 & 0 & C_1 & 0 & 0 \\ 0 & 0 & 0 & C_2 & 0 \\ 0 & 0 & 0 & 0 & L_{Load} \end{bmatrix} d/dt \begin{bmatrix} \tilde{i}_{L_1}(t) \\ \tilde{i}_{L_2}(t) \\ \tilde{v}_{C_1}(t) \\ \tilde{v}_{C_2}(t) \\ \tilde{i}_{Load}(t) \end{bmatrix} =$$

$$\begin{bmatrix} 0 & 0 & D_{ST} & -M_I & 0 \\ 0 & 0 & -M_I & D_{ST} & 0 \\ -D_{ST} & M_I & 0 & 0 & -M_I \\ M_I & -D_{ST} & 0 & 0 & -M_I \\ 0 & 0 & M_I & M_I & -R_{Load} \end{bmatrix}$$

$$\begin{bmatrix} \tilde{i}_{L_1}(t) \\ \tilde{i}_{L_2}(t) \\ \tilde{v}_{C_1}(t) \\ \tilde{v}_{C_2}(t) \\ \tilde{i}_{Load}(t) \end{bmatrix} + \begin{bmatrix} \mathrm{M_I} \\ \mathrm{M_I} \\ 0 \\ 0 \\ -\mathrm{M_I} \end{bmatrix} \tilde{\mathrm{v}}_{\mathrm{in}}(\mathrm{t}) +$$

$$\begin{bmatrix} V_{C_1} + V_{C_2} - V_{in} \\ V_{C_1} + V_{C_2} - V_{in} \\ -I_{L_1} - I_{L_2} + I_{load} \\ -I_{L_1} - I_{L_2} + I_{load} \\ -V_{C_1} - V_{C_2} + V_{in} \end{bmatrix} \tilde{d}_{ST}(t) \tag{29}$$

Now the Laplace form of equation (29) is written from equations (30)-34) as:

$$S\, L_1 \tilde{i}_{L_1} = D_{ST} \tilde{v}_{c_1}(s) - M_I \tilde{v}_{c_2}(s) + M_I \tilde{v}_{in}(s) + (V_{C_1} + V_{C_2} - V_{in}) \tilde{d}_{ST}(s) \tag{30}$$

$$S\, L_2 \tilde{i}_{L_2} = -M_I \tilde{v}_{c_1}(s) + D_{ST} \tilde{v}_{c_2}(s) + M_I \tilde{v}_{in}(s) + (V_{C_1} + V_{C_2} - V_{in}) \tilde{d}_{ST}(s) \tag{31}$$

$$S\, C_1 \tilde{v}_{c_1} = -D_{ST} \tilde{i}_{L_1}(s) + M_I \tilde{i}_{L_2}(s) - M_I \tilde{i}_{Load}(s) + (-I_{L_1} - I_{L_2} - I_{load}) \tilde{d}_{ST}(s) \tag{32}$$

$$S\, C_2 \tilde{v}_{c_2} = M_I \tilde{i}_{L_1}(s) - D_{ST} \tilde{i}_{L_2}(s) - M_I \tilde{i}_{Load}(s) + (-I_{L_1} - I_{L_2} + I_{load}) \tilde{d}_{ST}(s) \tag{33}$$

$$S\, L_{Load} \tilde{i}_{Load} = M_I \tilde{v}_{c_1}(s) + M_I \tilde{v}_{c_2}(s) - R_{Load} \tilde{i}_{Load}(s) - M_I \tilde{v}_{in}(s) + (-V_{C_1} - V_{C_2} + V_{in}) \tilde{d}_{ST}(s) \tag{34}$$

Since the ZSI impedance network is symmetrical, we can write:

- $L_1 = L_2 = L_{ZSI}$ and $C_1 = C_2 = C_{ZSI}$
- $i_{L_1}(t) = i_{L_2}(t) = i_L(t)$ and $v_{C_1}(t) = v_{C_2}(t) = v_C(t)$
- $I_{L_1} = I_{L_2} = I_L$ and $V_{C_1} = V_{C_2} = V_C$

Thus, equations (30) to (34) can be written as:

$$S\, L_{ZSI} \tilde{i}_L(s) = \left(D_{ST} - M_I\right) \tilde{v}_C(s) + M_I \tilde{v}_{in}(s) + (2V_C - V_{in})\, \tilde{d}_{ST}(s) \tag{35}$$

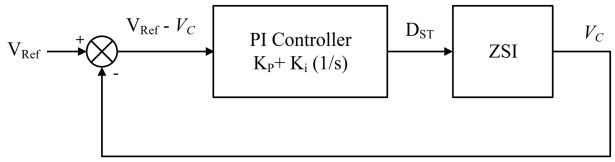

***Fig. 4**: Block diagram of ZSI with PI controller.*

$$S\,C_{ZSI}\tilde{v}_C(s) = \left(D_{ST} - M_I\right)\tilde{i}_L - M_I\tilde{i}_{Load}(s) + \left(2I_L - I_{Load}\right)\tilde{d}_{ST}(s) \tag{36}$$

$$S\,L_{Load}\tilde{i}_{Load}(s) = 2M_I\tilde{v}_C(s) - R_{Load}\tilde{i}_{Load}(s) - M_I\tilde{v}_{in}(s) + \left(2V_C - V_{in}\right)\tilde{d}_{ST}(s) \tag{37}$$

By analysing the steady-state equations and small signal, it is possible to determine the transfer functions at all specified operating points. Hence the transfer function to control output is shown in equation (38) [25]:

$$\begin{aligned} T_{\frac{v_C}{D_{ST}}}(s) &= \left.\frac{\tilde{v}_C(s)}{\tilde{D}_{ST}(s)}\right| at\ \tilde{v}_{in}(s) \\ &= \frac{\left(-2I_L + I_{Load}\right)L_{ZSI}L_{Load}\,s^2}{D_n} \\ &+ \frac{\left(\left(-2I_L + I_{Load}\right)L_{ZSI}R_{Load}\right)s}{D_n} \\ &+ \frac{\left(M_I\,V_{out}\,L_{ZSI} + \left(M_I - D_{ST}\right)V_{out}L_{Load}\right)S}{D_n} \\ &+ \frac{(M_I - D_{ST})V_{out}R_{Load}}{D_n} \end{aligned} \tag{38}$$

where,

$$\begin{aligned} &V_{out} = 2V_C - V_{in}\ and\ D_n = L_{ZSI}C_{ZSI}L_{Load}S^3 \\ &+ L_{ZSI}C_{ZSI}R_{Load}S^2 \\ &+ \left(2M_I^2L_{ZSI} + \left(D_{ST} - M_I\right)^2L_{Load}\right)S \\ &+ \left(D_{ST} - M_I\right)^2R_{Load} \end{aligned} \tag{39}$$

This PI controller generates switching pulses. Section 3 describes the modulation strategy for controlling the capacitor voltage as well as the dc-link boost voltage and creating the ST duty cycle. The typical modulation strategy is modified to acquire the transfer function of V_C/D_{ST} for the purpose of controller design.

5. WHALE OPTIMISATION TECHNIQUE

This paper expects to determine a PI controller parameter for controlled Modified ZSI. This section uses the WOA approach to optimise a controller parameter. The control strategy is presented in Fig. 4. The PI controller has the following form:

$$K_{PI}(s) = K_P + K_i\frac{1}{s} \tag{40}$$

where K_P is proportional gain and K_i is integration gain.

Considering the ST duty ratio (D_{ST}) as a ZSI control variable. This section of the article plans to optimise controller parameters ($K_P$and K_i) using WOA. A population-based meta-heuristic optimisation algorithm has two stages to the search process: exploitation and exploration. The proficiency of WOA is superior to a few other notable algorithms with regards to exploitation [26]. The WOA predominantly consists of three parts: encircle predation, bubble assault, and prey search.

A. *Encircle predation:* It is possible for humpback whales to encircle their prey and recognise its location. Once the best search agent has been identified, the other search agents will attempt to shift their positions in favour of it. The equations that follow show this behaviour:

$$\overline{D_1} = \left|\overline{C_1}.\,\overline{X^*}(k) - \overline{X}(k)\right| \tag{41}$$

$$\overline{X}(k+1) = \overline{X^*}(k) - \overline{A_1}.\,\overline{D_1} \tag{42}$$

The position vector X^* represents the best solution that has been found so far, $\overline{X}$ is the position vector. The updated position is represented by $\overline{X}(k+1)$ while the current position is represented by, $\overline{X}(k)$. k is the current iteration. $\overline{A_1}$ and $\overline{C_1}$ are coefficient vectors. $\overline{D_1}$ is the distance between the population's current members and random.

The following are the calculations for the vectors $\overline{A_1}$ and $\overline{C_1}$:

$$\overline{A_1} = 2\overline{a_1} \bullet \overline{rnd} - \overline{a_1} \tag{43}$$

$$\overline{C_1} = 2 \bullet \overline{rnd} \tag{44}$$

where $\overline{rnd}$ is a random number within the interval, and $\overline{a_1}$ is a number that diminishes straight from 2 to 0 during iteration.

B. *Bubble assault:* There are two methods for mathematically modelling the behaviour of humpback whales in the bubble net:

i. Shrinking encircling mechanism: In Equation (43), by decreasing the value of $\overline{a_1}$, this behaviour can be achieved. $\overline{A_1}$ will be an irregular worth in the stretch $[-a_1, a_1]$ where a_1 is diminished over the course of iterations from 2 to 0. The new place of a search agent can be characterised in any place between the agent's initial position and the place of the ongoing best agent by setting random qualities for $\overline{A_1}$ in [-1,1].

ii. Spiral updating position: To imitate humpback whales' helix-like movement, The position of the whale in relation to its prey is calculated in a spiral equation form:

$$\overline{X}(k+1) = \overline{D_1'} \bullet e^{bp} \bullet \cos(2\pi \mathrm{p}) + \overline{X^*}(k) \tag{45}$$

where $\overline{D_1'} = \left|\overline{X^*}(k) - \overline{X}(k)\right|$ is the separation between the prey (best solution attained so far) and the ith whale,

***Table 2**: Proposed System Parameters.*

Parameters	Value
Base Wind Speed	12 m/s
PMSG Speed	562 rpm
PMSG Electromagnetic Torque	4.16 Nm
Rectifier Filter Inductance	20 mH
Rectifier Filter Capacitance	10 mF

and p is a random number in the range [-1,1]. The logarithmic spiral's shape is determined by the constant b. The mathematical model is:

$$\overline{X}(k+1) = \begin{cases} \overline{X^*}(k) - \overline{A_1} \cdot \overline{D_1} & \text{if } l < 0.5 \\ \overline{D_1} \cdot e^{bp} \cdot \cos(2\pi p) + \overline{X^*}(k) & \text{if } l \geq 0.5 \end{cases} \quad (46)$$

where the random number p is found in [0,1].

C. *Prey search:* Based on the variation of the $\overline{A_1}$, the same strategy can be used for exploration. Authors use $\overline{A_1}$ with random values greater than 1 or less than -1 to force the search agent far from a reference whale. The mathematical model is:

$$\overline{D_1} = \left| \overline{C_1} . \overline{X_{rand}} - \overline{X} \right| \quad (47)$$

$$\overline{X}(k+1) = \overline{X_{rand}} - \overline{A_1} . \overline{D_1} \quad (48)$$

where $\overline{X_{rand}}$ is a whale chosen at random from the current population and represents a position vector of a randomly selected whale.

At each iteration, search agents adjust their positions in relation to either a randomly chosen search agent or the best solution that has been found so far. A random search agent is selected whenever $|\overline{A_1}|$ is greater than 1, and when $|\overline{A_1}|$ is less than 1, The best solution for updating the positions of the search agents is chosen. Depending on the value of l, WOA can move in either a spiral or a circular direction. The WOA algorithm is finished when a termination criterion is met. Fig. 5 depicts the WOA algorithm's flow chart.

6. RESULT AND DISCUSSION

In this work, WEGS model is designed with a modified ZSI model, providing controlled voltage output at the load canter. WEGS consists of the control system, wind turbine, PMSG, rectifier, and modified ZSI. A ZSI is used to adjust the voltage level between the PMSG and the load center, to the required level. A MATLAB/Simulink model is used to evaluate the suggested concept. Table 2 includes the simulation-related parameters:

The SB-PWM technique is provided to generate the ST pulses of ZSI. Table 3 indicates the modulation parameters.

Fig. 6 shows the generation of ST pulses with the help of reference sinusoidal waves, carrier triangular waves, and DC lines. As a result, the ZSI can raise the voltage to the desired AC output voltage.

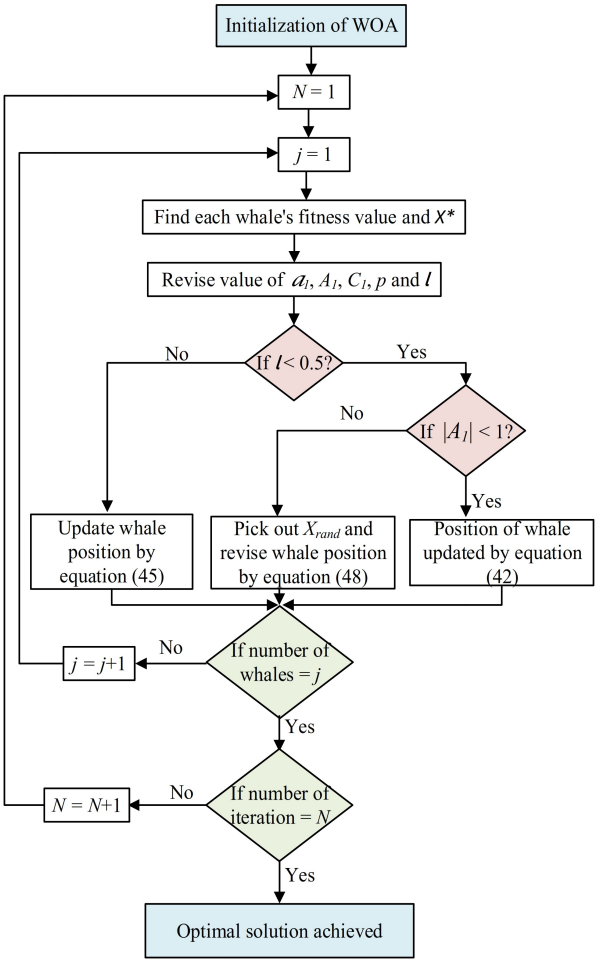

***Fig. 5**: The WOA flowchart.*

***Table 3**: Modulation Parameters.*

Parameters	Value
Reference Wave Amplitude	17.5 V
Carrier Wave Amplitude	25 V
Modulation Index, M_I	0.7
Duty Ratio for ZSI, D_{ST}	0.3
Boost Factor, B_{ZSI}	2.5

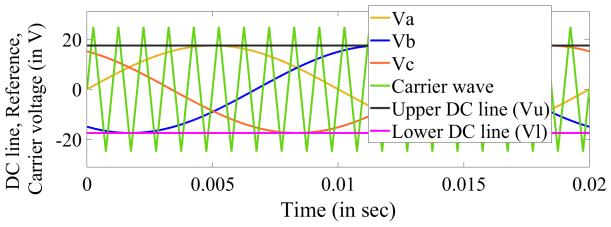

***Fig. 6**: Switching pattern in SB-PWM technique.*

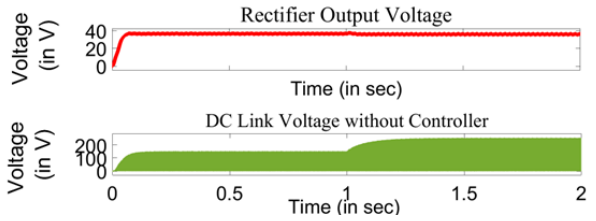

(a) Input DC voltage and DC link voltage.

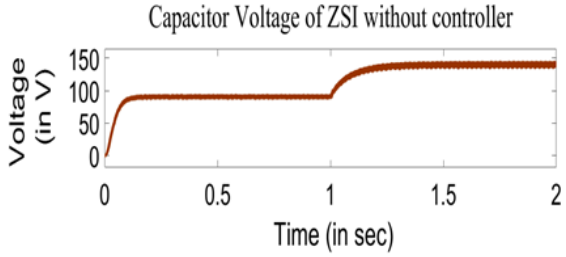

(b) Capacitor voltage

***Fig. 7**: Conventional ZSI input DC voltage, capacitor voltage and DC link voltage.*

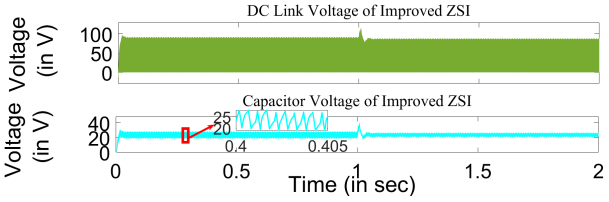

***Fig. 8**: Modified ZSI DC link voltage and capacitor voltage.*

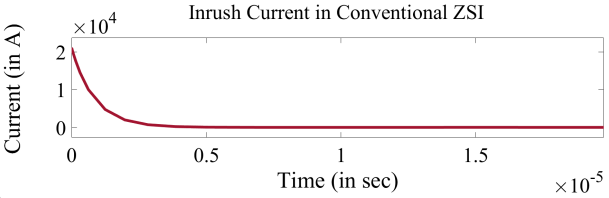

***Fig. 9**: Conventional ZSI inrush current.*

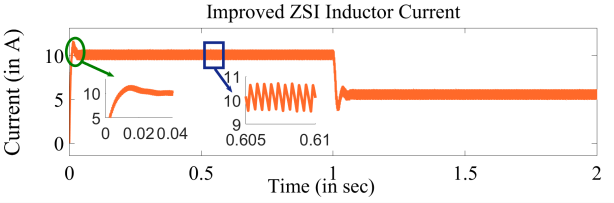

***Fig. 10**: Modified ZSI model inductor current.*

6.1 Comparison of Traditional ZSI Model with Modified ZSI Model

Both the conventional model and the modified model of the ZSI-based WEGS system are examined. The same power switches and diodes are used in both. Table 4 indicates the criteria used to compare the advantages of the modified ZSI and the conventional one.

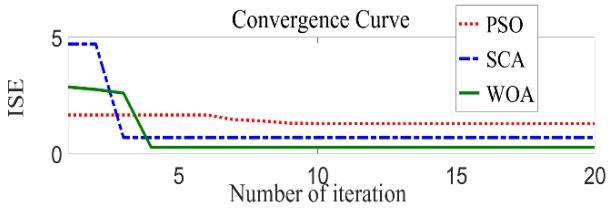

***Fig. 11**: Convergence curve graph for various algorithms tested for the suggested system.*

***Table 4**: Conventional and modified model ZSI simulation parameters and simulation results.*

Parameters	Conventional ZSI	Modified ZSI
Input Voltage, V_{in}	36 V	36 V
Duty Ratio, D_{ST}	0.3	0.3
Load Resistance, R_{Load}	10 Ω	10 Ω
Load Inductance, L_{Load}	1 mH	1 mH
ZSI Network Capacitor Voltage, V_C	90 V	27 V
DC Link Voltage of ZSI, V_{DC}	150 V	90 V
Output Voltage per phase, V_{Load}	56 V	63 V
Output Current per phase, i_{Load}	5.6 A	6.3 A

The ZSI model's input DC voltage is the same as the rectifier's output voltage. The capacitor voltage for conventional ZSI is shown in equation (49) and for modified ZSI is shown in equation (50).

$$V_{C(Traditional\ ZSI)} = \frac{1}{1-2D_{ST}}\, V_{in} \tag{49}$$

$$V_{C(Improved\ ZSI)} = \frac{D_{ST}}{1-2D_{ST}}\, V_{in} \tag{50}$$

The modified topology's Z-source capacitor voltage V_C is equal to zero when the shoot-through duty ratio D_{ST} is zero, as shown by equation (50). V_C is inherently zero when the converter is soft-starting. Controlling the gradual D_{ST} increase from zero can help to make a smooth start. Nevertheless, this is not the case in conventional topology. Fig. 7 and Fig. 8 illustrate simulation results that supports the theoretical findings.

Fig. 7(b) and Fig. 8's capacitor voltage waveforms demonstrate that the conventional ZSI model experiences significant capacitor voltage stress; however, in the modified ZSI model, the capacitor voltage is always less than the input voltage supplied to the inverter. Fig. 8 subplot depicts the capacitor voltage ripple (ΔV_C) used to compute the ZSI network capacitance (C_{ZSI}) value, as expressed in equation (1). Also, the new ZSI model has a far lower inrush current than the traditional ZSI model, as shown in Fig. 10 and Fig. 9, respectively.

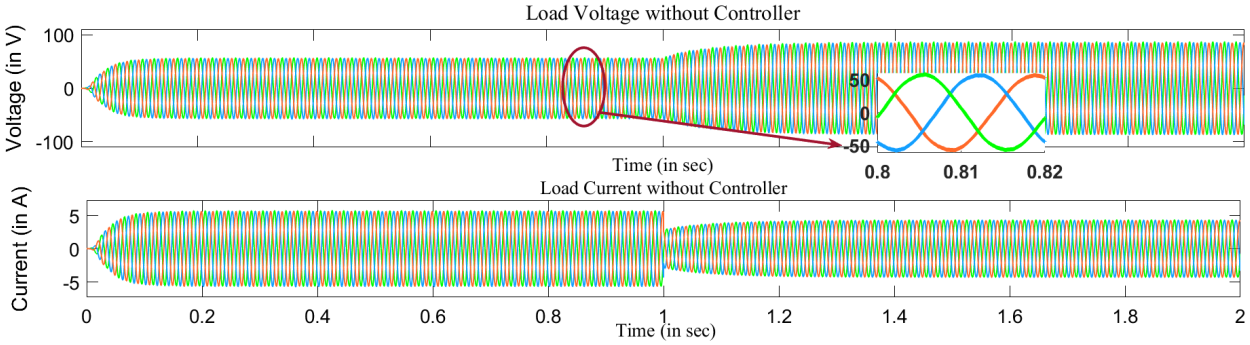

***Fig. 12**: Output voltage and current waveforms of the WEGS system without a controller.*

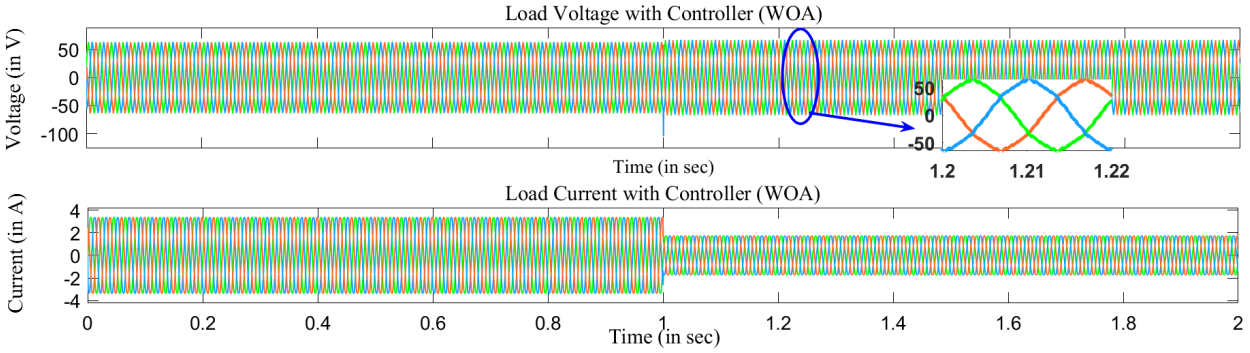

***Fig. 13**: Output voltage and current waveforms of the WEGS system with an optimised controller.*

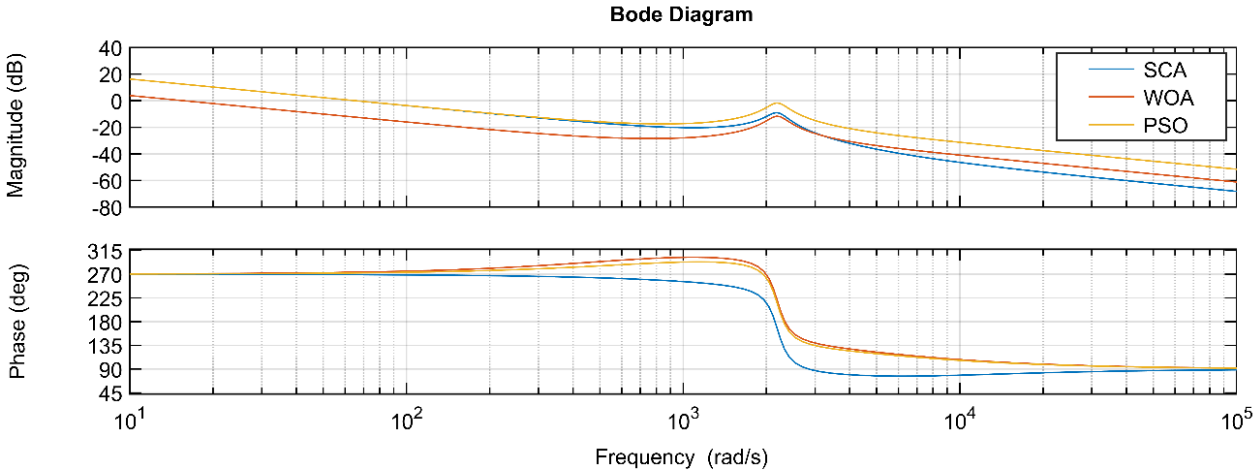

***Fig. 14**: Bode plot for closed-loop modified ZSI with different algorithms.*

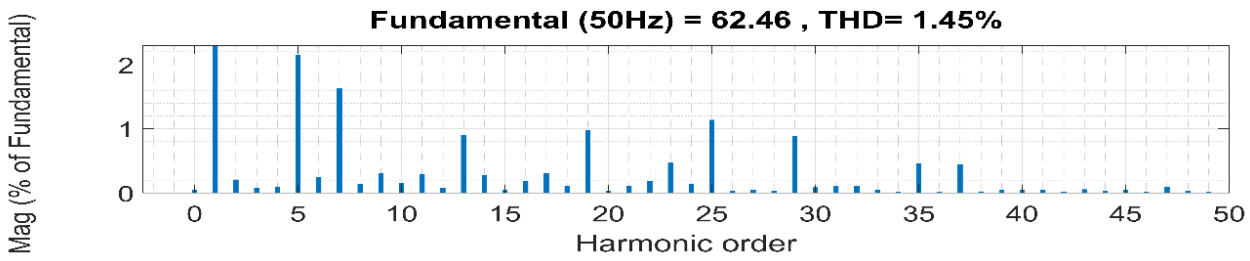

***Fig. 15**: FFT analysis of output voltage (for a single-phase) waveform with a controller.*

***Table 5**: Stability margin of the close loop ZSI system based on different algorithms.*

Algorithms	GM	PM
WOA	13.9	90.9
SCA	9.11	89.1
PSO	3.34	92.3

The ZSI network inductance (L_{ZSI}) value for no resonance, as defined in equation (2), is calculated using the inductor current ripple (i_L) shown in Fig. 10 inductor current subgraph, which represents the system's soft start.

6.2 WOA for PI Controller

The integral square error (ISE) of the system objective function for the controller varying with iterations is shown in Fig. 11. The results show that of PSO, SCA, and WOA, WOA is the most suitable for the proposed model as it converges more accurately with each iteration. The error function, which was initially defined as an ISE, was reduced to around 0.26 throughout the optimisation phase with WOA.

Fig. 12 depicts the WEGS' output voltage and current waveforms without a PI controller, while Fig. 20 depicts the output graph with a WOA-based PI controller. The simulation result for the RL load of resistance 10 ohms and inductance 1 mH, which is adjusted to 20 ohms and 2 mH after 1 second of simulation time is shown. Fig. 12 shows that after 1 second of simulation (when the load changes), the modified ZSI's output voltage increases and the current decreases with an increased load, whereas Fig. 13 shows that the modified ZSI's output voltage nearly remains the same even though the load causes the device's output current to decrease after increasing the RL load value. The output waveform demonstrates that the designed controller meets the requirement to produce the obligatory AC voltage of 63 V for the variable AC loads. The goal of this section is to present the results of optimised controller parameters for a three-phase modified ZSI system using a WOA-based technique, for fixed output voltage with varying RL-load. Whereas, without a controller, the system functions only on the input signal and the properties of the components. With a controller, the system adds additional processing steps, such as feedback control, which might cause nonlinearities or distortions in the waveform.

The ZSI system is linearized with a controller, and the study of bode plots is used to further confirm the superiority of WOA along with convergence curve. The PSO, SCA, and WOA's bode plots are compared in Fig. 14, and their relative gain margin (GM) and phase margin (PM) are listed in Table 5. The suggested approach's superiority is established by comparing the Bode plots of the different algorithm.

6.3 Output waveform's THD analysis

By using the SB-PWM modulation technique, the WEGS system's output waveform has a very low (1.45%) harmonic content, as shown by Fig. 15 Fast Fourier Transform (FFT) of the output voltage waveform.

7. CONCLUSION

The main goal of this work was closed-loop control of a modified ZSI using the capacitor voltage control technique. It is possible to simulate closed-loop control of a three-phase RL load fed by a modified ZSI based WEGS, using a PI controller. A thorough small signal model of the ZSI is developed using the RL load. The ZSI system's non-linear structure makes it challenging to design the PI controller's parameters. In this work, the WOA optimisation method has thus been suggested. Traditional ZSI problems are outlined and examined. Based on the outcomes of both theoretical studies and simulations, we can draw the following conclusions:

- A good soft-start strategy can lessen inductors' inrush current for modified topology.
- The voltage stress on the Z-source capacitor is significantly decreased in order to obtain the same boost capability.
- The closed-loop control of the Z-source inverter enables real-time feedback and modification.
- It has been noted that in comparison with PSO and SCA-based PI controllers for ZSI, the WOA-designed PI controller yields more satisfying results.
- WEGS and other new energy applications will make substantial use of the WOA optimisation technique with the suggested upgraded topology.
- The integration of WEGS with modified ZSI may enable features such as peak shaving or grid support functions, increasing the power conversion system's flexibility and dependability. This could lead to novel solutions to address the specific needs of variable load systems or grid systems.

REFERENCES

[1] D. Kumar, R. K. Nema, S. Gupta, and N. K. Dewangan, "Development of Open Switch Fault-Tolerant Capability in CCS-MLI Topology," *ECTI Transactions on Electrical Engineering, Electronics, and Communications*, vol. 20, no. 2, pp. 197–205, Jun 2022.

[2] V. Rathore, D. Kumar, and P. Mundra, "A Symmetrical Cross-Connected T-Type Multilevel Inverter With Reduce Device Count," *ECTI Transactions on Electrical Engineering, Electronics, and Communications*, vol. 21, no. 2, pp. 1–12, Jun 2023.

[3] S. Kumari, R. K. Mandal, and D. Verma, "Three-Phase Space Vector Modulated Improved Z-Source Inverter," *2nd International Conference on Power Energy, Environment, and Intelligent Control (PEEIC)*, pp. 249–253, 2020.

[4] O. Ellabban and H. Abu-Rub, "Z-Source Inverter:

Topology Improvements Review," *IEEE Industrial Electronics Magazine*, vol. 10, no. 1, pp. 6–24, 2016.

[5] Y. P. Siwakoti, F. Z. Peng, F. Blaabjerg, P. C. Loh, G. E. Town, and S. Yang, "Impedance-source networks for electric power conversion part II: Review of control and modulation techniques," *IEEE Transactions on Power Electronics*, vol. 30, no. 4, pp. 1887–1906, 2015.

[6] R. M. Malathi R., "Comparison of PV based Embedded Z-Source Inverter fed Three Phase Induction Motor with PI Controller and PID Controller based closed loop systems," *Third International Conference on Advances in Electrical, Electronics, Information, Communication and Bio-Informatics (AEEIC)*, pp. 142-146, 2017.

[7] G. Shiva, K. Hrishikes, and R. Issan Raj, "Closed Loop Voltage mode control of Impedance Source Inverter (ZSI)," *International Conference on Emerging Trends in VLSI, Embedded System, Nano Electronics and Telecommunication System (ICEVENT)*, pp. 1-5, 2013.

[8] S. Kumaravel and V. Thomas, "Performance Analysis of a Z-Source Inverter with Controller for Autonomous System Application," *IEEE 7th International Conference on Power and Energy (PECon)*, pp. 355–359, 2018.

[9] A. R. Yılmaz, B. Erol, A. Delibaşı, and B. Erkmen, "Design of gain-scheduling PID controllers for Z-source inverter using iterative reduction-based heuristic algorithms," *Simulation Modelling Practice and Theory*, vol. 94, pp. 162–176, 2019.

[10] R. A. Krohling and J. P. Rey, "Design of Optimal Disturbance Rejection PID Controllers Using Genetic Algorithms," *IEEE Transactions on Evolutionary computation*, vol. 5, no. 1, pp. 78–82, 2001.

[11] J. S. Chiou, S. H. Tsai, and M. T. Liu, "A PSO-based adaptive fuzzy PID-controllers," *Simulation Modelling Practice and Theory*, vol. 26, pp. 49–59, 2012.

[12] P. B. De Moura Oliveira, "Modern heuristics review for PID control systems optimization: A teaching experiment," de Moura Oliveira, P. "Modern heuristics review for PID control." *6th International PhD workshop on systems and control: a young generation viewpoint*, pp. 828–833, 2005.

[13] U. Raj, "Optimally enhanced fractional-order cascaded integral derivative tilt controller for improved load frequency control incorporating renewable energy sources and electric vehicle," *Soft Computing*, vol. 3, 2023.

[14] [14] F. Marini and B. Walczak, "Particle swarm optimization (PSO). A tutorial," *Chemometrics and Intelligent Laboratory Systems*, vol. 149, pp. 153–165, 2015.

[15] S. Yousaf, A. Mughees, M. G. Khan, A. A. Amin, and M. Adnan, "A comparative analysis of various controller techniques for optimal control of smart nano-grid using GA and PSO algorithms," *IEEE Access*, vol. 8, pp. 205696–205711, 2020.

[16] M. Wang and G. Lu, "A Modified Sine Cosine Algorithm for Solving Optimization Problems," *IEEE Access*, vol. 9, pp. 27434–27450, 2021.

[17] H. R. Al-Faisal, I. Ahmad, A. A. Salman, and M. G. Alfailakawi, "Adaptation of Population Size in Sine Cosine Algorithm," *IEEE Access*, vol. 9, pp. 25258–25277, 2021.

[18] S. Kumaravel and V. Thomas, "Performance Analysis of a Z-Source Inverter with Controller for Autonomous System Application," *IEEE 7th International Conference on Power and Energy (PECon)*, pp. 355–359, 2018.

[19] G. Shiva, K. Hrishikes, and R. I. Raj, "Closed loop voltage mode control of impedance source inverter (ZSI)," *Embedded System, Nano Electronics and Telecommunication System (ICEVENT)*, pp. 1-5, 2013.

[20] Y. Tang, S. Xie, C. Zhang, and Z. Xu, "Improved Z-source inverter with reduced Z-source capacitor voltage stress and soft-start capability," *IEEE Transactions on Power Electronics*, vol. 24, no. 2, pp. 409–415, 2009.

[21] S. Kumari and R. K. Mandal, "Study of shoot-through control pulse generation for a Z-source converter with wind turbine energy system," *Engineering Research Express*, vol. 4, no. 3, p.035035, 2022.

[22] M. M. S. Kharat, Diksha Murlidhar, "Solar PV fed Proposed Simple Boost Controlled Z- source Inverter for Grid," *International Conference on Recent Advances and Innovations in Engineering (ICRAIE)*, pp. 1–5, 2020.

[23] M. Amirbande, M. S. Zarbil, D. Frp, D. Lxvw, and D. F. Lu, "Simple Boost Control of a New High Voltage Gain Z- Source Inverter," *Power Electronic and Drive Systems and Technologies Conference (PEDSTC)*, pp. 169–173, 2018.

[24] L. J. Rashad, "Mathematical Model and Analysis of the Z-Source Inverter," *European Journal of Electrical Engineering and Computer Science*, vol. 4, no. 1, 2020.

[25] A. R. Yilmaz, B. Erol, A. Delibaşı, and B. Erkmen, "Design of gain-scheduling PID controllers for Z-source inverter using iterative reduction-based heuristic algorithms," *Simulation Modelling Practice and Theory*, vol. 94, pp. 162–176, 2019.

[26] S. Chakraborty, A. Kumar, S. Sharma, and S. Mirjalili, "A novel enhanced whale optimization algorithm for global optimization," *Computers & Industrial Engineering*, vol. 153, 2021.

Sweta Kumari received her B.Tech. degree from Aryabhatta Knowledge University, Bihar, India, in 2013 and M.tech. degree from National Institute of Technology (NIT) Patna, India, in 2017. She is currently pursuing Ph.D from National Institute of Technology (NIT) Patna, India. She is about 5 years of teaching experience. She is currently working as an assistant professor in Government Engineering College Siwan, Bihar. Her research interest includes renewable sources of energy, power electronic converters and control of power electronic devices.

Rajib Kumar Mandal received his B. E. degree from MACT Bhopal, M. E. degree from Jadavpur University, India, and Ph. D. from NIT Patna, India in the year 1999, 2004, and 2018 respectively. He is currently working as an associate professor in NIT Patna. His area of interest includes power systems, power electronics, multilevel inverters, and renewable energy sources.